J. Fluid Mech. (1975), *vol.* 68, *part* 4, *pp.* 673–693
Printed in Great Britain

The distortion of turbulence by general uniform irrotational strain

By A. J. REYNOLDS

Department of Mechanical Engineering, Brunel University, Uxbridge, Middlesex, England

AND H. J. TUCKER

Department of Mechanical Engineering, University of Windsor, Ontario

(Received 8 May 1974)

This paper describes the measured response of grid turbulence to three limiting types of uniform homogeneous strain: plane straining, axisymmetric elongation and axisymmetric flattening. Straining was achieved by allowing the turbulence to be convected through suitable distorting ducts; the maximum strain ratios were 5·8, 6·0 and 2·3, respectively. An attempt is made, using rapid-distortion theory, to specify an effective strain which accounts for the initial anisotropy of the grid turbulence; in the experiments, this effect was most important for the third species of strain. The maximum effective strain ratios were calculated as 4·05, 7·2 and 2·75, respectively. The rapid-distortion results are able to describe several features of the response of the turbulence with good accuracy: (i) the variation of total turbulence energy through the experimental ducts; (ii) the tendency of one component (that in the direction of the (larger) negative strain) to contain one-half of the turbulence energy after only moderate straining; and (iii) the changes in dimensionless structure parameters composed of ratios of component intensities. The first kind of prediction requires that the concurrent decay be specified in a simple way; (ii) and (iii) require that the initial anisotropy be taken into account. The predictions (iii) are generally less accurate than the others. The degree of success achieved by the rapid-distortion hypothesis is rather surprising, since the strain rates in the experiments were not as large as those for which the theory might have been expected to be valid. It is concluded that successful models of turbulence must provide a vorticity amplification essentially like that of rapid-distortion theory. However, the simple distorting flows considered here may not provide severe tests of more refined models, since many features of the response have already been accounted for.

1. Introduction

The experiments reported here extend an earlier study (Tucker & Reynolds 1968) of the response of grid turbulence to irrotational plane strain which is uniform in space and time. In the earlier experiments straining was achieved in two ways: (i) by passing the turbulence-bearing fluid through a distorting channel whose cross-sectional area remained constant, while the height and width varied;

and (ii) by passing the fluid through a contracting duct of constant height but varying width. Here a more general class of ducts in which the height, width and cross-sectional area all may vary will be considered. In this way a broad class of irrotational uniform distortions can be established. Of course, if the cross-section were to expand rapidly, the flow would separate from the walls, and the proposed pattern of straining would not be set up. However, this behaviour can be avoided by arranging that the cross-sectional area decreases along the duct. Since continuity dictates that at least one of the strains be positive for small density changes, no loss in generality is occasioned by this practical restriction, provided that the strain type is not required to change dramatically along the channel.

Thus we appear to be in a position to determine experimentally the response of grid turbulence to any uniform irrotational pattern of strain. While this information is not directly applicable to flows of wide practical interest, it does provide tests for various theories of turbulence, and is a source of empirical input for models of turbulence. In particular, Townsend (1956, pp. 81–83) has postulated a particular pattern of 'equilibrium' response to various types of straining, and these experiments go some way towards filling in the gaps in the information available to him.

As was noted above, the turbulence strained in these experiments was that produced by a nominally uniform grid; this has the effect of modifying the strains achieved in the tests. As is well known, the turbulence generated by passing a fluid through a grid is not isotropic, though it is usually very nearly axisymmetric. Consequently, it might be considered that the turbulence which approaches the distorting ducts of our tests has already experienced a certain effective straining. We shall see later than the effect of this initial anisotropy is to limit the range of strain types set up in our tests.

While most of the experiments on uniformly strained homogeneous turbulence have used irrotational strain (MacPhail 1944; Townsend 1954; Maréchal 1967*a*, *b*, 1972; Tucker & Reynolds 1968; and the present work), a few attempts have been made to study the response of turbulence to a uniform shear flow where the fluid experiences rotation as well as extension and compression (Rose 1970; Champagne, Harris, & Corrsin 1970). Although this latter situation is more difficult to establish, it is somewhat closer to practically important turbulent flows. However, in these the mean straining is, typically, not only rotational, but also non-uniform in space and time.

Another line of investigation related to this work is the theoretical study of 'rapidly distorted' turbulence by Taylor (1935), Ribner & Tucker (1953), Batchelor & Proudman (1954), Pearson (1959), Deissler (1961, 1970) and Fox (1964), among others. The last few of these workers have included the effects of viscosity in their calculations; since inertial interactions are neglected in rapid-distortion theory, the inclusion of viscosity implies that the Reynolds number of the turbulence is very low indeed. The theory has been applied to various practical problems by Uberoi (1956), Deissler (1963, 1966, 1967), Mills & Corrsin (1959), Hunt (1973) and Hunt & Mulhearn (1973).

With the availability of experimental data describing the actual response of turbulence to uniform straining, as reported in the penultimate paragraph, it

has been possible to improve upon the rapid-distortion model. This has been attempted by Rotta (1962), Townsend (1970) and Lumley (1970). These experimental results have also been incorporated into apparently more general analytical models of turbulence, for example, Harlow & Romero (1969), the thin-flow model of Hanjalić & Launder (1972) and the ν-fluid model of Proudman (1970) and Dowden (1972, 1974).

In this paper we shall make comparisons between our measurements and the results of rapid-distortion theory. In doing this, we remain aware of the severe limitations of this model, and do not seek to imply that it is capable of wide application. Our reasons for using this theory as a basis for comparison are as follows. First, it has been used in this way in earlier reports of uniform-distortion experiments, and our use of it will facilitate comparisons with that work. Second, the rapid-distortion results are obtained relatively easily from assumptions that are explicit and widely known. Finally, the applications of the rapid-distortion model are of some importance, and an indication of its validity is therefore of interest.

In making comparisons between our measurements and this simple model of response to straining, we shall use the rapid-distortion results to allow for the initial anisotropy of grid turbulence (typically, $u'/v' = 1{\cdot}2$, where u' and v' are streamwise and cross-stream r.m.s. values). The theory easily yields explicit predictions for the case of initially isotropic turbulence, and we shall adopt a simple stratagem, to be explained below, in order to apply these results to a specified initial turbulence, while avoiding the numerical integrations required in evaluating the full results for initially anisotropic turbulence. These integrations would require one either to have available accurate measured spectra relating to the particular turbulence, or to postulate spectra of plausible form. It is our *opinion* that the component intensities obtained by integration would be relatively insensitive to the details of the spectra, but the demonstration, or refutation, of this opinion would require extensive calculations.

The stratagem we adopt is to consider the structure at the entry to the distorting duct to be the result of the application of hypothetical strains l_{ih} to a hypothetical isotropic turbulence. For actual strain ratios l_i the theoretical results (for initial isotropy) with which comparisons are appropriate are those for the effective strains

$$l_{ie} = l_{ih} l_i \tag{1}$$

(no summation with respect to the indices i is intended).

The detailed formulae developed by Ribner & Tucker (for axisymmetric contraction) and by Batchelor & Proudman (for arbitrary distortion) are given in Tucker (1970) and will not be reproduced here. A number of features of distorted, initially isotropic turbulence will be presented in figure 3 of the present paper, and the corrections incorporated in (1) can be made using such curves. For a measured initial degree of anisotropy, the hypothetical strains l_{ih} are read from graphs. Then for a station within the duct at which the actual strains are l_i, predictions are obtained by reading values corresponding to $l_{ie} = l_{ih} l_i$.

The plotted results also prove useful in suggesting the degree of straining required to establish invariant, or only slowly changing, structure of the strained

turbulence. However, this aspect of the response depends on the type of straining applied, and we shall defer our consideration of these predictions until a type parameter for the strain has been introduced.

2. The classification and generation of strains

For irrotational straining the mean rate-of-strain tensor may be given as

$$\{E_{ij}\} = (\partial U_1/\partial x_1)\begin{bmatrix} 1 & 0 & 0 \\ 0 & F & 0 \\ 0 & 0 & -1-F \end{bmatrix} \tag{2}$$

on introducing the type parameter for the strain

$$F = \frac{\partial U_2/\partial x_2}{\partial U_1/\partial x_1}.$$

This is a constant for uniform distortion, among other constant-type strain patterns. The constant-density continuity requirement $\partial U_i/\partial x_i = 0$ has been satisfied by taking

$$\partial U_3/\partial x_3 = -\partial U_1/\partial x_1 - \partial U_2/\partial x_2 = -(1+F)\,\partial U_1/\partial x_1.$$

As in Tucker & Reynolds (1968) the axes will be chosen such that

$$\partial U_1/\partial x_1 > 0, \quad 1 \geqslant F \geqslant -1-F. \tag{3}$$

Thus the strain rate $\partial U_1/\partial x_1$ always represents an extension, while $\partial U_3/\partial x_3$ always represents a compression; the third normal strain may be either an extension or compression. The entire range of strain types is encompassed by

$$1 \geqslant F \geqslant -\tfrac{1}{2}. \tag{4}$$

In order to prevent separation of the flow from the duct walls, it is expedient to arrange that x_1 (or possibly x_2) is along the axis of the channel.

For $F = 0$ we obtain plane strain, for $F < 1$ we have an elongation of the fluid elements and for $F > 1$ we have a flattening of the elements. The case of plane strain has been given considerable attention already, and we shall deal with the two extreme departures from it: $F = -\frac{1}{2}$, the elongation achieved in a symmetrical contraction of the turbulence-convecting flow; and $F = 1$, a flattening equivalent to symmetrical diffusion of the flow. The first of these situations arises in the contracting sections found in test channels such as wind tunnels, and has been studied by Uberoi (1956). The second case, of two extending strains and one compression, arises in diffusing channels, but the avoidance of separation and large losses dictates that the strain rate be rather small; moreover, the mean strain pattern is usually non-uniform and rotational. Hence we must seek an alternative way of generating the strain pattern $F = 1$.

The two channel forms in which the required strain fields were established are shown in figures 1 and 2. The mean streamlines in uniformly distorting flow ($\partial U_1/\partial x_1$, etc., constants) are given by

$$\left.\begin{aligned} x_2 &\propto (x_1 + \text{constant})^F, \\ x_3 &\propto (x_1 + \text{constant})^{-1-F} \end{aligned}\right\} \tag{5}$$

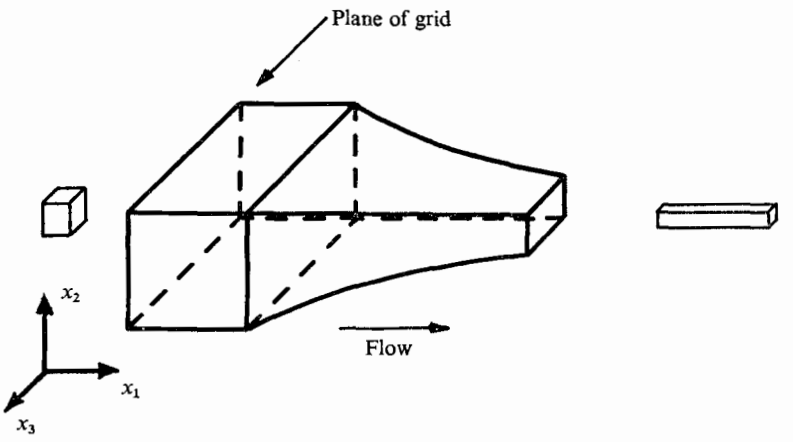

FIGURE 1. Form of contracting duct in which symmetric elongation was achieved. This is duct 1 of table 1 *et seq.*, with strain-type parameter $F = -\frac{1}{2}$.

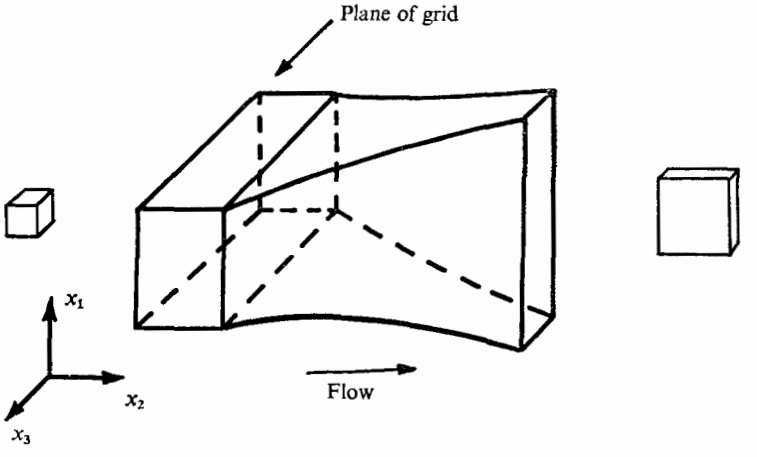

FIGURE 2. Form of contracting duct in which symmetric flattening was achieved. This is duct 4 of table 1 *et seq.*, with strain-type parameter $F = 1$.

when the axis of the duct is in the x_1 direction, and by

$$\left.\begin{aligned} x_1 &\propto (x_2 + \text{constant})^{1/F}, \\ x_3 &\propto (x_2 + \text{constant})^{-1-1/F} \end{aligned}\right\} \tag{6}$$

when the duct axis is in the x_2 direction. These results give the ideal shape of the channel walls, although in practice some correction, either through analytical prediction or through empirical adjustment, may be required to establish a required mean velocity field in the central part of the channel. The spreading of boundary layers into the flow sets a limit on the length of the duct and hence on the intensity of uniform strain that can be generated in given test conditions.

In addition to the type parameter F, two further dimensionless quantities are required to specify a particular mode of application of uniform strain: a measure

Duct form	Sketch	Strain-type parameter F	Maximum strain $l_{1\max}$	Strain-rate parameter I
1. Symmetric, elongating contraction	Present figure 1	$-\frac{1}{2}$	5·8	0·95
2. Plane contraction	Previous figure 2	0	5·4 2·8	0·97 0·32
3. Plane distortion	Previous figure 1	0	6·0	0·32
4. Symmetric, flattening contraction	Present figure 2	1	2·3	0·25

TABLE 1. Experimental conditions

of the total strain and a measure of the rate of application of strain relative to some rate of reaction of the turbulence. For the former we shall use

$$l_1 = t\,\partial U_1/\partial x_1, \tag{7}$$

the largest of the strain ratios, t being the time over which the strain has been applied. As a measure of the relative rate of straining, we shall use

$$I = t_d/t_s = (\partial U_1/\partial x_1)\left[\frac{-\overline{q^2}}{d\overline{q^2}/dt}\right]_0, \tag{8}$$

where $t_s = (\partial U_1/\partial x_1)^{-1}$ is the time scale characterizing the strain application and $t_d = [-\overline{q^2}/(d\overline{q^2}/dt)]_0$ is the time scale for decay of the turbulence at the beginning of the distortion.

Table 1 shows the leading features of the tests, data for the plane-strain experiments being included to facilitate comparisons; the experimental arrangements are described in more detail in Tucker (1970). In each case the length of the distorting section was 8·0 ft, and it began 2 ft downstream of the turbulence-generating grid. The inlet section of the distorting tunnel (figure 1 of Tucker & Reynolds 1968) was 45 in. by $7\frac{1}{2}$ in. and the inlet section of each contracting duct was 30 in. by 17 in. The values of the parameter I relate to a grid formed of perforated steel sheet, 0·030 in. thick, with bars $\frac{3}{16}$ in. wide and a square mesh of scale $M = \frac{11}{16}$ in. All the tests were carried out in normal atmospheric air: For the contractions $U = 20$ ft/s at the mesh ($Re_M = 6780$) and at the entrance to the straining section; for the distorting duct, constant axial velocities of $U_2 = 20$ and 40 ft/s were established.

The distortions $F = 1, -\frac{1}{2}$ were obtained by modifying the contracting duct used earlier to achieve plane strain. Liners of appropriate shape were fixed to the flat top and bottom of the channel, the flexible sides being adjusted to fit the liners using adjusting screws. The allowance for boundary-layer growth mentioned above may be made either analytically, at the design stage, or by trial and error, during the experiments. The former method is appropriate when the duct has rigid walls, as does the laterally distorting duct 3, but for the flexible-walled channels of interest here, an adjustment is possible to make the rate of distortion uniform along the channel. In any case the strain rates quoted were obtained from velocity measurements made under test conditions, and not from design calcula-

Duct	Hypothetical strains		Maximum strains		Strain-type parameters	
	l_{1h}	l_{2h}	$l_{1\max}$	$l_{1e\max}$	F	F_e
1	0·7	1·2	5·8	4·05	$-\frac{1}{2}$	−0·50
2	0·7	1·2	5·4	3·78	0	0·14
3	1·2	0·7	6·0	7·20	0	−0·18
4	1·2	0·7	2·3	2·75	1	0·47

TABLE 2. Hypothetical and effective strains

tions. The strain rates were measured using plots exemplified by figures A1 and A2 of our earlier paper.

In the experiments considered here, the distortion was applied in different ways relative to the axis of the duct and of the initial anisotropy of the grid turbulence. Thus the structure established after straining represents not only the planned distortion, but also a variable contribution from the initial state of the turbulence. A somewhat more meaningful comparison of the responses to different strain types may be obtained by identifying the response with the effective strains which take into account the initial anisotropy. These are something like the strains which would have to be applied in each case to convert initially isotropic turbulence to the observed final form.

Equation (1) shows how this reinterpretation can be made. For the grid and preliminary duct geometry to which table 1 relates, the initial anisotropy was taken to be given by $\overline{u^2}/\overline{q^2} \simeq 0{\cdot}42, \quad \overline{v^2}/\overline{q^2} = \overline{w^2}/\overline{q^2} \simeq 0{\cdot}29$ (9*a*)

for all the ducts, where u is the axial velocity fluctuation and v and w are the cross-stream components. The rapid-distortion results give the hypothetical strains

$$l_{1h} = 0{\cdot}70, \quad l_{2h} = l_{3h} = 1{\cdot}20 \tag{9b}$$

corresponding to the application of a mild axisymmetric deceleration to the stream carrying the hypothetical isotropic turbulence.

The selection of the initial degree of anisotropy (9*a*) is not entirely straightforward: some variation occurs even during simple decay; the straining extends some way into the upstream duct where the flow is nominally parallel; and there is, of course, some experimental scatter. All the experiments reported here were carried out with the same kind of grid, and most with the same blower tunnel supplying the distorting duct. Hence the turbulence may be expected to be much the same at the start of each pattern of straining. Our measurements indicated initial values of $\overline{u^2}/\overline{q^2}$ between 0·41 and 0·43, when an attempt was made to allow for the variable upstream influence of the straining sections. We have adopted the central value as that most likely to hold for all the experiments.

The significance of the values (9*a*) for axes referred to the strains is indicated in the second and third columns of table 2. Using (1) we can find the effective strain ratios, the maximum value of l_{ie} being that given in the table. For uniform distortion the type parameter is related to the strain ratios through

$$F = \frac{\partial U_2/\partial x_2}{\partial U_1/\partial x_1} = \frac{\log l_2}{\log l_1}. \tag{10}$$

Hence the effective value of the type parameter is given by

$$F_e = \frac{\log l_{2e}}{\log l_{1e}} = \frac{F + \log l_{2h}/\log l_1}{1 + \log l_{1h}/\log l_1}. \tag{11}$$

This parameter changes as the intensity of straining increases. The initial value is simply

$$F_e = \log l_{2h}/\log l_{1h} = -0{\cdot}5 \quad \text{or} \quad -2{\cdot}0.$$

The final values for the several ducts are given in the last column of table 2.

Only for duct 4 is the final value of the effective type parameter dramatically different from the nominal value defined by the duct geometry. For this case the hypothetical and actual strains are of very different character, and the final value of the latter is rather small. Looked at in this way, our experiments are seen not to cover the entire range of strain types or, alternatively, not to cover the entire range of initial conditions. For the existing degree of initial anisotropy, a very large strain ratio would be required to approach the limit $F_e = 1$. For example, $l_{1\max} = 10$, with $F = 1$, would give the final value $F_e = 0{\cdot}78$. Alternatively, one might adopt the stratagem of Comte-Bellot & Corrsin (1966), and introduce a preliminary contraction to render $\overline{u^2} = \overline{v^2} = \overline{w^2}$ before the major straining was applied. Of course, this procedure, like our analytical treatment, which assumes a hypothetical isotropic turbulence, is based upon the simplistic view that all departures from isotropy are manifested in and controllable through the ratio of the component intensities.

3. Experimental results

3.1. *Characterization of response*

The primary description of the response of the turbulence to strain will be through the ratios $\overline{u_1^2}/\overline{q^2}$, $\overline{u_2^2}/\overline{q^2}$ and $\overline{u_3^2}/\overline{q^2}$, in which the effect of decay is suppressed so that direct comparisons are possible with rapid-distortion results which do not allow for viscosity. These ratios can be combined in a number of ways to form other dimensionless measures of the structure of the turbulence; to facilitate comparisons with plane-strain experiments, we shall adopt a parameter which has been used to describe them:

$$K = (\overline{u_3^2} - \overline{u_1^2})/(\overline{u_3^2} + \overline{u_1^2}). \tag{12}$$

The way in which the axes have been selected ensures that, for large strains, $\overline{u_3^2}$ is the largest intensity and $\overline{u_1^2}$ the smallest.

According to rapid-distortion theory, the structure parameters K, $\overline{u_1^2}/\overline{q^2}$, etc., depend on the strain ratio l_1 and the type parameter F. Figure 3 indicates the variations for the case of initial isotropy. Note that the predictions for $F = 0$ and $-\frac{1}{2}$ are not very different. This behaviour is typical of other measures of response, and follows from the rapid reduction of the energy of the smallest component by the application of either of these two types of strain. Note too that the amount of strain required to 'saturate' the response is least for $F = 1$. Thus the design values of l_1 given in table 1 would appear to be large enough,

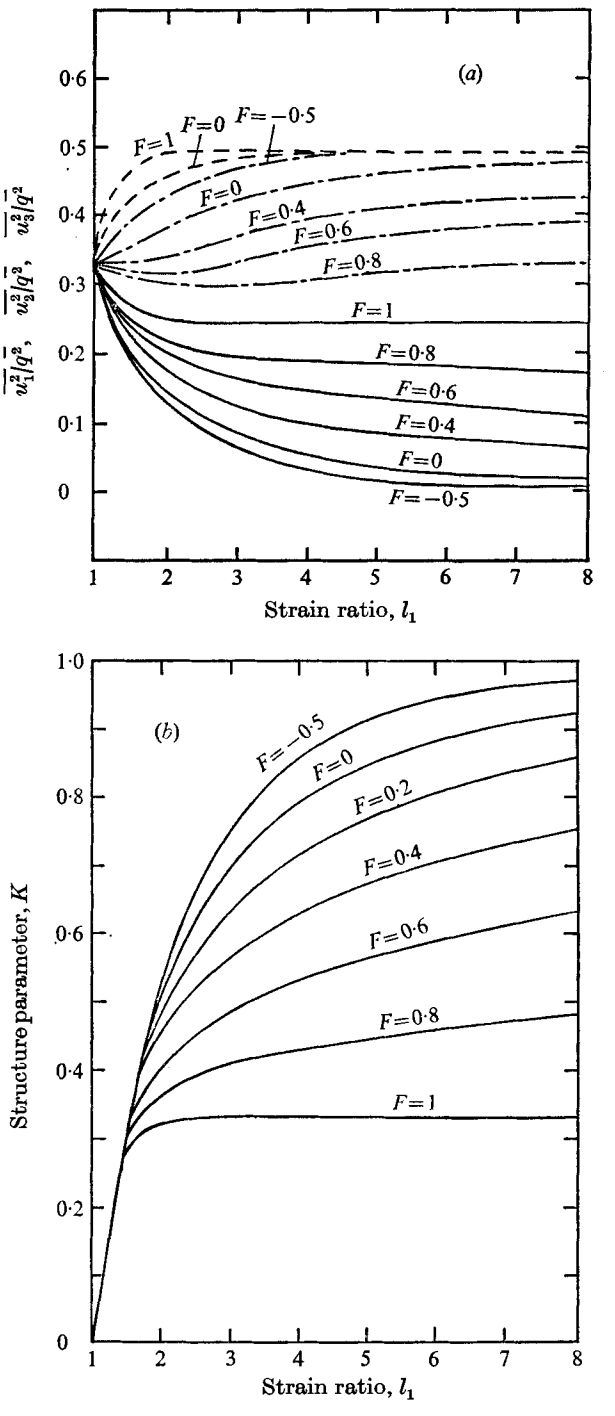

FIGURE 3. Dependence of response of initially isotropic turbulence on total strain ratio l_1 and strain-type parameter F. (*a*) Distribution of turbulence energy among the components: ——, $\overline{u_1^2}/\overline{q^2}$; – – – –, $\overline{u_2^2}/\overline{q^2}$; – – – –, $\overline{u_3^2}/\overline{q^2}$. The limiting curves apply to the components on both sides. (*b*) Variation of the structure parameter K defined in (12).

on the basis of rapid-distortion theory, to achieve a close approach to the 'equilibrium' structure for each type of strain. On the other hand, consideration of the effective values given in table 2 ($l_1 = 4{\cdot}05$ for $F_e = -0{\cdot}50$ and $l_1 = 2{\cdot}75$ for $F_e = 0{\cdot}47$) suggests that the final structure may be some way from equilibrium, particularly for the strain specified nominally by $F = 1$. This is yet another way in which the initial anisotropy of the strained turbulence complicates the interpretation of measurements of this kind. Of course, factors not taken into account in the rapid-distortion model – viscosity and higher-order interactions – will also influence the rate at which 'equilibrium' is approached or, indeed, may prevent any such state from coming into existence.

In Tucker & Reynolds (1968) the response in the distorting channel was described using relative intensities such as $\overline{u_1^2}/U_2^2$, where U_2 is the nominally uniform mean axial velocity. Such parameters are less meaningful and less convenient for experiments in which the convection velocity varies systematically along the duct. However, one important conclusion did emerge when this kind of presentation was used in the earlier paper: the variation of the total turbulence energy $\frac{1}{2}\overline{q^2}$ can be predicted with good accuracy ($\pm 10\,\%$, say) throughout the distorting channel, provided that rapid-distortion theory is corrected for decay using the simple assumption that the rate of decay is not changed by the straining. This kind of correction was proposed by Ribner & Tucker (1953). The conclusion remains valid for the turbulence in the contracting ducts of the present experiments. In general, the decay correction is not as successful in predicting the variation of the individual intensities, and this fact is reflected in differences between measured and predicted values of $\overline{u_1^2}/\overline{q^2}$, etc., which will be discussed later.

3.2. *Subsidiary results*

Before considering the main body of tests, we shall note some supporting results that are dealt with in more detail by Tucker (1970).

Frequency spectra for the intensities $\overline{u_1^2}$, etc., were measured in the various ducts, and one-dimensional wavenumber spectra were calculated from them using Taylor's hypothesis. The general nature of the modifications to the spectra by straining is that suggested by rapid-distortion theory; see, for example, Townsend (1954). The spectral components of the low-energy component of the turbulence are relatively larger at higher wavenumbers, indicating that the strain-induced anisotropy is less marked in the smaller elements of the turbulence.

As a preliminary to the decay correction referred to above, the decay of the individual components and of the total energy in uniform convection was studied for different grids and flow velocities. It was found that

$$\overline{q^2} \propto (x - x_0)^{-p} \quad \text{with} \quad p = 1{\cdot}24,\ 1{\cdot}29,$$

$$\overline{u^2} \propto (x - x_0)^{-n} \quad \text{with} \quad n = 1{\cdot}35,\ 1{\cdot}35,$$

$$\overline{v^2} = \overline{w^2} \propto (x - x_0)^{-m} \quad \text{with} \quad m = 1{\cdot}17,\ 1{\cdot}22.$$

The first of each pair of indices refers to the square-mesh grid described in connexion with table 1; the second set of figures refers to a grid made from 0·037 in.

'expanded' aluminium sheet, with a diamond mesh with diagonals 1·19 in. and 0·60 in. and bars of width 0·09 in. For these two grids $x_0/M \simeq 5$. A survey was made of the values of the decay constants found by other workers.

The signals from slanting hot-wire anemometers were interpreted, as explained in Tucker & Reynolds (1968), by assuming a directional dependence of the form

$$E^2 = A + B(U \sin\theta)^C.$$

The constant C was found to lie in the range $0{\cdot}42 \pm 0{\cdot}03$. In reducing the results, the value 0·45 was adopted, as this gave results virtually indistinguishable from those provided by the individual measured values of C. The other constants, A and $B \sin^C\theta$, were found by calibration in developed pipe flow. Several comparisons were made with results obtained using the directional dependence

$$E^2 = A + BU^2(\sin^2\theta + k^2\cos^2\theta)^{\frac{1}{2}C}$$

with $k = 0{\cdot}2$ and a measured value for θ. The values obtained in these two ways were not very different, but those based on direct calibration were somewhat more convincing.

3.3. *Correction of hot-wire signals*

For the low turbulence levels of these tests, significant contamination of the output from the hot-wire anemometers was provided by high frequency instrument noise and by rather low frequency background turbulence in the blower tunnel which supplied the contracting ducts. This was the case, in particular, when the sensor was located near the exit from the duct, where decay had reduced the intensity of the grid turbulence.

The background turbulence (that found in the absence of a grid) at the entrance to the contracting ducts was around

$$u'/U, \quad v'/U, \quad w'/U = 0{\cdot}005 \pm 0{\cdot}001.$$

The component u'/U remained roughly constant through the ducts but other components fell until, typically,

$$v'/U, \quad w'/U = 0{\cdot}002$$

at the exit. The different behaviour of the streamwise component is reasonable if the background activity has an important contribution from plane sound waves generated by the fan upstream. Attempts to reduce this contamination using additional screens failed.

All of the turbulence intensities reported here have been corrected by the following procedure, which will be referred to as method I.

(i) The signals were passed through a 20 kHz low-pass filter to remove a large part of the instrument noise.

(ii) From each mean-square fluctuation in voltage was subtracted the value measured at the same location in the same duct when no grid was present.

The second step is justified if the grid turbulence and background turbulence are independent and if the former is not influenced by the grid. These conditions should be met if the background turbulence consists of low frequency sound waves travelling along the duct.

Some use was also made of another method of correction, based on the observation that some 80 % of the background energy lay below 20 Hz. In this method, method II, signals were passed through both a 20 kHz low-pass filter and a 20 Hz high-pass filter before the background value (also subjected to this dual filtering) was subtracted. Values obtained using method II are shown in the following figures using solid, rather than open, symbols. After surveying the test results, we shall consider the relative merits of the two methods of correction.

3.4. *Response to straining*

In Tucker & Reynolds (1968) attention was concentrated on results for plane straining in the laterally distorting tunnel, measurements in the contracting duct being introduced only as supporting evidence. We begin our consideration of the main body of tests in the contracting ducts by examining results obtained in the plane-strain channel (duct 2 of tables 1 and 2). Figures 4(*a*) and (*b*) show the distribution of energy among the three components for the two strain ratios indicated in table 1: $l_{1\max} = 5{\cdot}4$ and $2{\cdot}8$. Figure 5 gives the corresponding values of K for these two straining conditions, for which $I = 0{\cdot}97$ and $0{\cdot}32$, respectively. For strain ratios $l_1 < 4$, say, the rapid-distortion predictions (modified to account for the initial state of the turbulence) are remarkably successful in describing these decay-insensitive parameters. Note, however, that the theory is not as successful for the laterally distorting duct (duct 3 of tables 1 and 2), which also produces $F = 0$, nominally. This is evident in figure 4 of Tucker & Reynolds (1968), and becomes even clearer when comparison is made with predictions which allow for initial anisotropy.

Figures 6 and 7 give corresponding results for the symmetrical contraction (duct 1 of tables 1 and 2). Here the theory is less successful, departing markedly from the measured values for $l_1 > 2$, say. Figure 7 shows also a value measured by Uberoi (1956) in an axisymmetric contraction. While the variation of the strain-rate parameter I in the present tests is not large enough to reveal the influence of this parameter on the response ($I = 0{\cdot}25$–$0{\cdot}97$ only), Uberoi's result was obtained for $I = 5{\cdot}0$, and lies close to the rapid-distortion prediction. This difference between our results and Uberoi's is that which would be expected, for the arguments of the rapid-distortion model suggest that it will be applicable when $I \gg 1$. While our tests do not satisfy this criterion (and the degree of agreement which is achieved is therefore somewhat surprising), Uberoi's experiment is not too far from doing so.

The response to the final type of strain, the flattening distortion $F = 1$ (duct 4 of tables 1 and 2), is presented in figures 8 and 9. Here the theory is fairly successful over the whole of the range of strains, though this is rather small.

Let us now consider the effect of using method II to correct for background turbulence; values obtained in this way are shown in figures 4(*a*) and 5 ($F = 0$), 6 and 7 ($F = -\frac{1}{2}$), and 8 and 9 ($F = 1$). The results for $F = 0$ are nearly the same as those obtained using method I. The changes for $F = -\frac{1}{2}$ are somewhat larger, particularly for the smallest component, and tend to move the measurements closer to the rapid-distortion predictions. The effect of method II on the results for $F = 1$ is even more significant, the measured values being moved a little

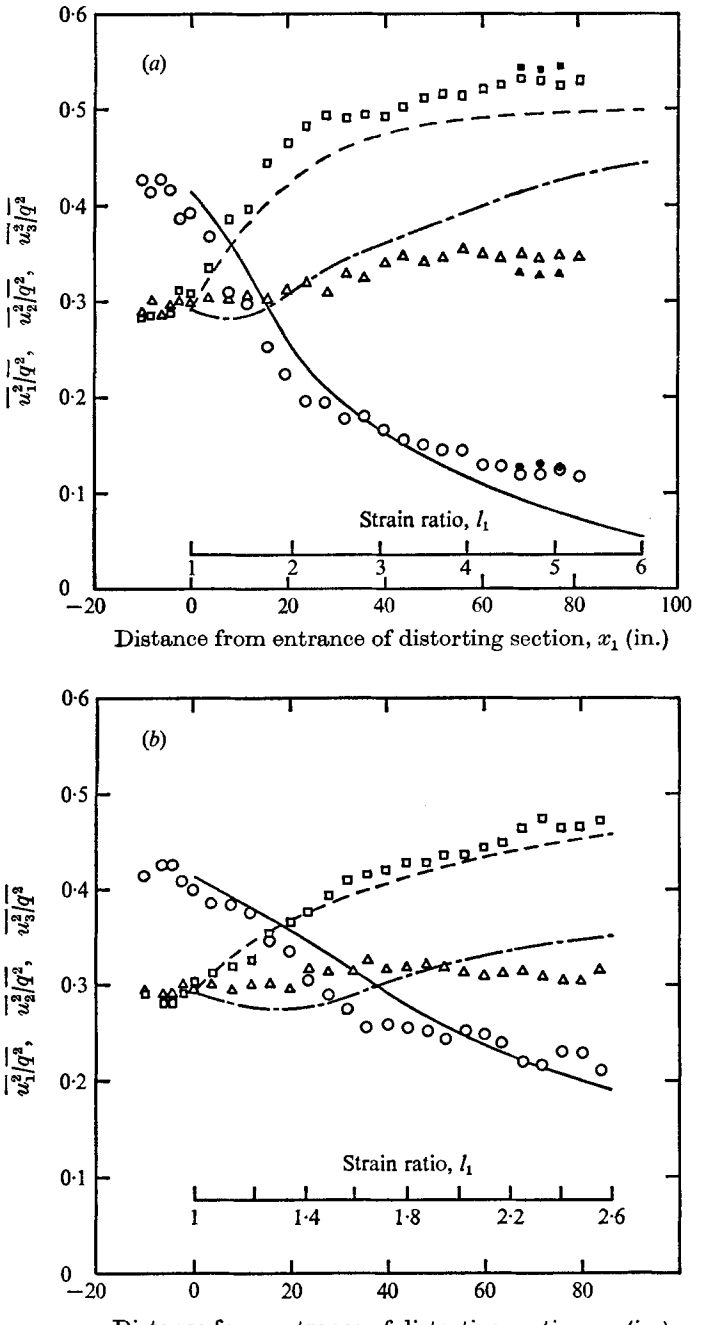

FIGURE 4. Variation of relative intensities in plane strain ($F = 0$, duct 2) for (*a*) $l_{1\max} = 5{\cdot}4$ and (*b*) $l_{1\max} = 2{\cdot}8$. The curves were obtained from the rapid-distortion results of figure 3. The solid points were obtained using the filtering technique termed method II.

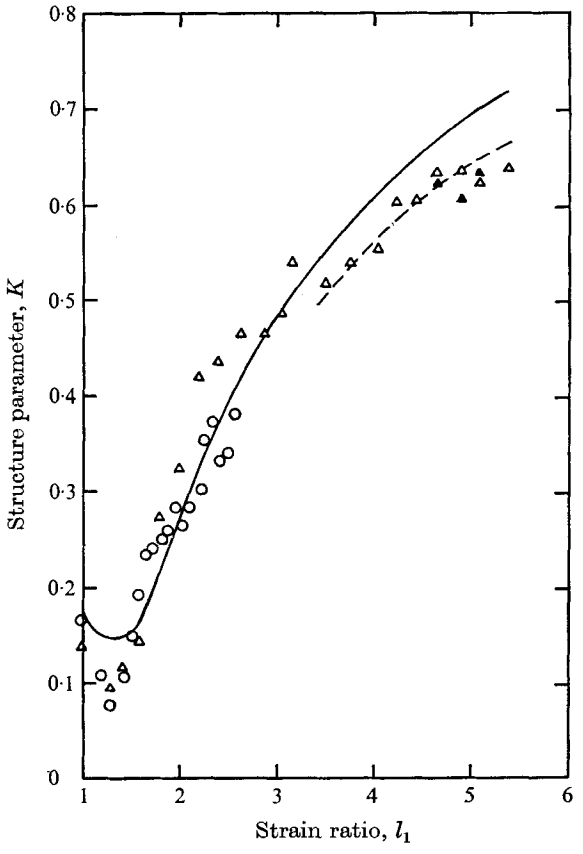

FIGURE 5. Comparison of the values of the structure parameter K measured in plane strain ($F = 0$, duct 2). △, maximum strain ratio $l_{1\max} = 5{\cdot}4$, strain-rate parameter $I = 0{\cdot}97$; ○, $l_{1\max} = 2{\cdot}8$, $I = 0{\cdot}32$; ——, rapid-distortion theory of figure 3; — —, equation (13).

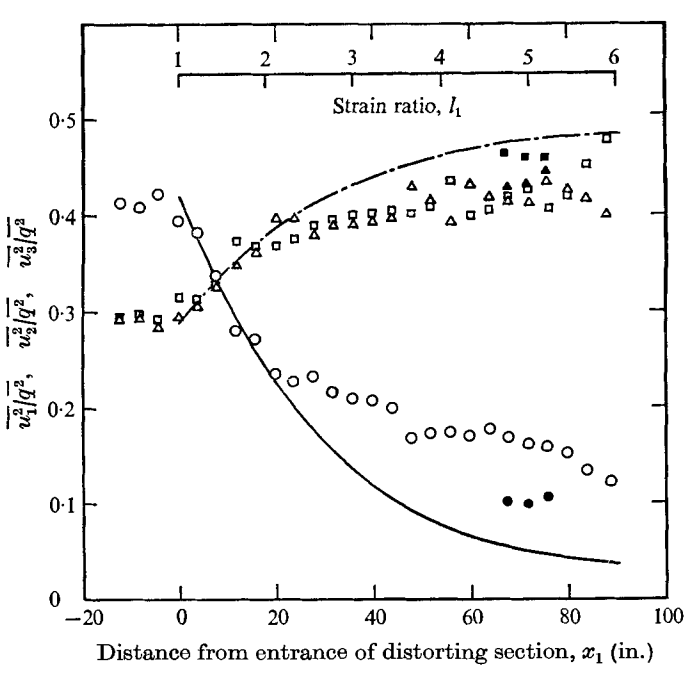

FIGURE 6. Variation of relative intensities in axisymmetric elongation ($F = -\frac{1}{2}$, duct 1). The curves are given by the rapid-distortion results of figure 3.

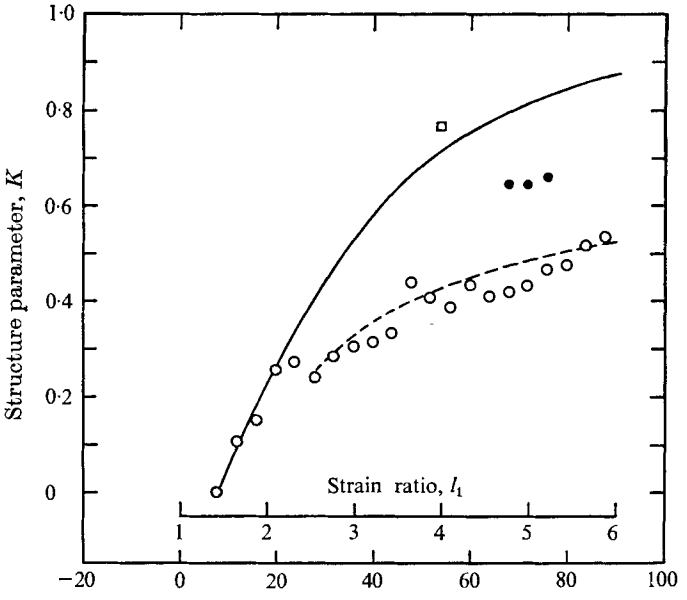

FIGURE 7. Variation of the structure parameter K corresponding to figure 6. ——, rapid-distortion theory; ——, equation (13); □, from measurements of Uberoi (1956).

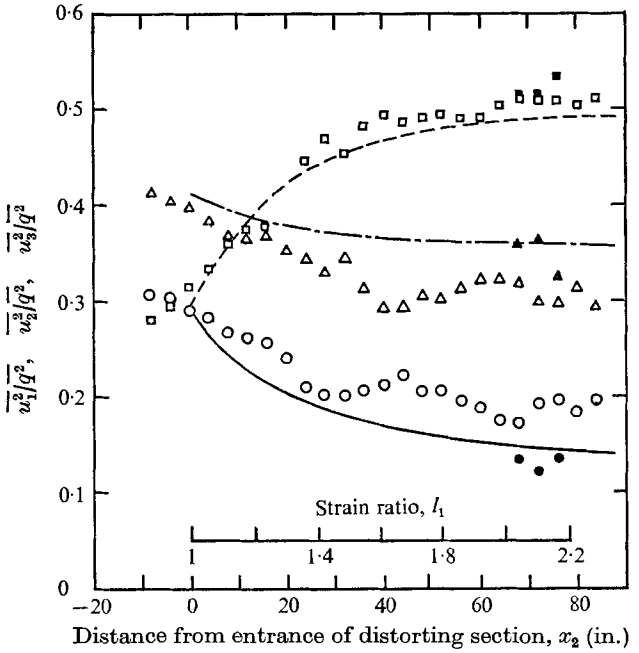

FIGURE 8. Variation of the relative intensities in axisymmetric flattening ($F = 1$, duct 4). The curves are given by rapid-distortion theory.

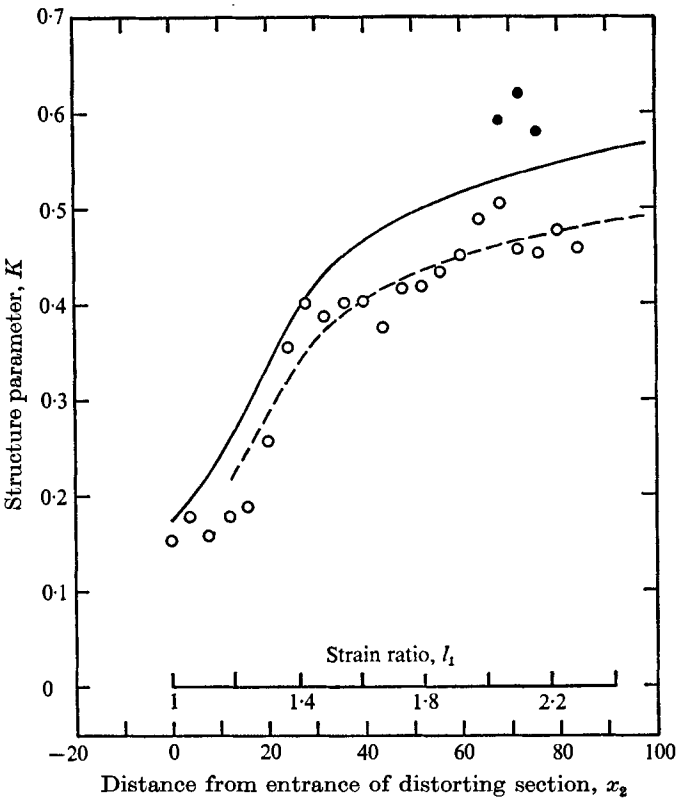

FIGURE 9. Variation of the structure parameter K corresponding to figure 8. ——, rapid-distortion theory; — —, equation (13).

beyond the theoretical predictions. These last changes are implausible, and this casts doubt on method II for other situations.

Looking over the three sets of results, we see that the changes in the parameter K are generally somewhat less than those predicted. However, the measured variations $K(l_1)$ have much the same form as the predicted curves $K_t(l_1)$ and may be represented with good accuracy by

$$K/K_t = C, \tag{13}$$

where $C(<1)$ is a constant for each strain type. The values of this constant which give the dashed curves in figures 5, 7 and 9 are shown in table 3, together with the value appropriate to the distorting duct (duct 3), which was found in the same way. The least values of l_1 for which these linear relationships hold are also shown; for smaller values of l_1 the agreement between K and K_t is better than that indicated by table 3. Values of the strain-rate parameter I are also given in table 3, but there is no obvious relationship between them and the value of C.

Table 4 indicates the final distributions of energy among the components, those values attained near the ends of the four experimental channels. In pre-

Duct	C of (13)	l_1	I
1	0·63	> 1·4	0·95
2	0·93	> 3·5	0·97, 0·32
3	0·63	> 1·3	0·32
4	0·86	> 2·3	0·25

TABLE 3. Relationship between measured response and that predicted by rapid-distortion theory

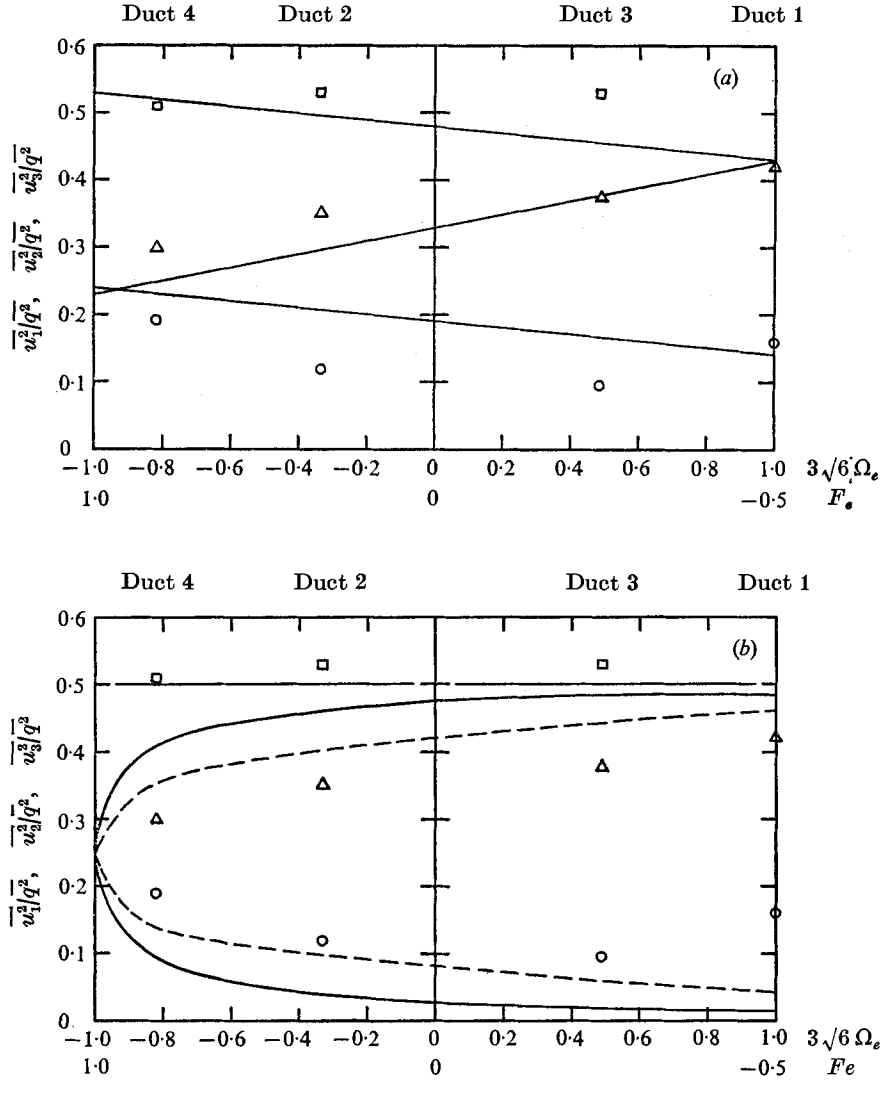

FIGURE 10. Final values of relative intensities as functions of effective value Ω_e of Townsend's strain parameter [equation (14)] and effective type parameter F_e [equation (11)]. (*a*) Comparison with linear variations proposed by Townsend (1956). (*b*) Comparison with rapid-distortion predictions: ——, $l_1 = 6$; — —, $l_1 = 3$.

F	F_e	$3\sqrt{6}\,\Omega_e$	$\overline{u_3^2}/\overline{q^2}$	$\overline{u_2^2}/\overline{q^2}$	$\overline{u_1^2}/\overline{q^2}$
$-\frac{1}{2}$	$-0{\cdot}50$	1	0·42	0·42	0·16
0	0·14	$-0{\cdot}33$	0·53	0·35	0·12
0	$-0{\cdot}18$	0·49	0·53	0·375	0·095
1	0·47	$-0{\cdot}82$	0·51	0·31	0·19

TABLE 4. Final values of the intensity parameters

senting these graphically in figure 10, we use an alternative strain parameter which was introduced by Townsend (1956, p. 81):

$$\Omega = \frac{s_1 s_2 s_3}{(s_1^2+s_2^2+s_3^2)^{\frac{3}{2}}} = \frac{-F(1+F)}{2^{\frac{3}{2}}[1+F(1+F)]^{\frac{3}{2}}}, \tag{14}$$

where $s_1 = \partial U_1/\partial x_1$, etc. are the mean strain rates. This parameter varies from $\Omega = 1/3\sqrt{6}$ to 0 to $-1/3\sqrt{6}$ when the type parameter F varies from $-\frac{1}{2}$ to 0 to 1.

In figure 10(*a*) the results of table 4 are plotted with the linear variations proposed by Townsend; Ω_e is the value of Ω found using F_e. The final values obtained in Townsend's (1954) plane-strain experiments lie at the intersections of these lines with the axis $F = 0$; they are 0·19, 0·33 and 0·48. Townsend supposed the grid turbulence of his experiments to be isotropic prior to straining, but it is apparent from figure 10 that the strain parameter is very sensitive to initial anisotropy near $F = 0$. Moreover, as was seen in Tucker & Reynolds (1968), the straining was not severe enough to bring the turbulence close to the equilibrium condition.

Proudman (1970) was able to reproduce Townsend's values of the intensities for $F = -\frac{1}{2}$, 0 and 1 using a ν-fluid representation of a turbulent fluid. These results, like Townsend's empirical proposals, are in rather poor agreement with experiment, save for $F \simeq 1$ or $-\frac{1}{2}$. However, Dowden (1972, 1974) has since shown that the behaviour of ν-fluids can be made consistent with measurements made in homogeneous strain fields.

In figure 10(*b*) the results of table 4 are plotted with the predictions of rapid-distortion theory for $l_1 = 3$ and 6, values which span the ranges of nominal and effective strains given in table 2. The most striking feature of the results is the correctness of the rapid-distortion prediction that $\overline{u_3^2}/\overline{q^2} \simeq \frac{1}{2}$ for all but the smallest strains. This prediction fails (and then not too badly) only when $F \simeq -\frac{1}{2}$, that is, when there is no largest component because $u_2' \simeq u_3'$. Moreover, the results of Uberoi (1956), and the present measurements when corrected for background turbulence using method II, give $\overline{u_2^2}$ and $\overline{u_3^2}$ closer to $\frac{1}{2}\overline{q^2}$ and a correspondingly smaller value of $\overline{u_1^2}$.

The theory is not as successful in predicting the lesser components; not unexpectedly, these are more nearly equal than the predictions would suggest. However, the rapid-distortion model does indicate the general shape of the dependence upon strain type, the curves being bowed rather than straight as Townsend was forced to assume in the absence of experimental data.

Duct	Strain-type parameter	K	
		Method I	Method II
1	$-\frac{1}{2}$	0·54	0·65
2	0	0·64	0·63
3	0	0·62	0·62
4	1	0·50	0·62

TABLE 5. Final values of the structure parameter K

Since a good deal of attention has in the past been given to the magnitude of the parameter K, the highest values achieved in our tests are listed in table 5, for measurements obtained using correction methods I and II. For every strain type values in excess of $K = 0{\cdot}5$ were attained, and for some, values in excess of $K = 0{\cdot}6$. There is no reason to suppose that higher values are impossible. In this connexion it is interesting to note that Dowden (1974) used his ν-fluid model of response, which had been shown to be capable of representing the measurements in duct 3 with good accuracy, to predict the response to continued straining of this type. He found that K rose to a value around 0·8 when straining had been carried on some $2\frac{1}{2}$ times as long as it was in the experimental channel. An asymptotic or equilibrium structure was approached when the straining had proceeded for about three times as long as in the tests.

4. Concluding remarks

The dominant feature of the response to every type of irrotational strain is the tendency of the largest of the turbulence components to acquire one-half of the total turbulence energy. A close approach to this condition is usually (the case of axisymmetric contraction excepted) attained when the maximum strain ratio is about two ($l_1 \simeq 2$). Unfortunately, this simple fact about the response to irrotational strain cannot be carried over to shear flows, where the axes of strain rotate relative to the strained fluid and the length scales of the larger elements of the turbulence are usually comparable with the length scale of the strain pattern. Moreover, in wall-bounded flows the constraint of the wall ensures that the normal fluctuation component is small, and this overrides the simple amplification observed in irrotational straining. In fact, in wall turbulence the largest of the principal mixing stresses often contains well over half of the kinetic energy of the turbulence.

Rapid-distortion theory gives the total turbulence energy with fair accuracy (within 10 %, say) provided that allowance is made for the decay which proceeds while straining takes place. In some cases the theory is also successful in predicting the component intensities (within 20 %, say), but in others it is markedly less accurate. These successes of the simplest response theory are not very important in themselves, for more sophisticated models of response have recently been developed. However, the degree of success which has been achieved does suggest two conclusions of wider significance: (i) more comprehensive models of turbulence must incorporate a vorticity-amplification process essentially like

that of rapid-distortion theory; and (ii) the uniform-strain flows considered here may not provide very severe tests of turbulence models, since the rapid-distortion hypothesis already accounts for most features of the response.

The rapid-distortion results indicate (see figure 3*a*) that dimensionless parameters such as $\overline{u_1^2}/\overline{q^2}$ will achieve nearly uniform values for $l_1 < 6$, and sometimes ($F \simeq 1$) for $l_1 < 2$. However, these structure parameters usually continued to change throughout our experiments. Hence the anisotropy parameter K, which rose to the range 0·5–0·7 in the experiments, may be expected to take on even higher values if larger strains are applied. However, the results of figure 3(*b*) suggest that a reduction in K may be produced by larger strains of the type $F \simeq 1$, since the ultimate value of K falls (in this model) as the effective value F_e rises towards the nominal value F.

Although the range of strain rates achieved here was not sufficient to demonstrate that different equilibrium structures are approached when large strains are achieved at different rates, comparisons with the results of Uberoi suggest that this is in fact the case. This implies that a true equilibrium structure can be attained, if at all, only when the time scales of the turbulence and of the strain vary in the same way along the distorting channel, so that the local value of $I = t_d/t_s$ remains constant during straining.

The influence of the initial state of the strained turbulence – to be precise, its departure from isotropy – is so large that it must be taken into account if meaningful comparisons are to be made with theoretical predictions, in particular, those of rapid-distortion theory. Initial anisotropy also has implications for the design of straining experiments of the kind reported here, since in applying strain in different ways relative to the axis (or axes) of anisotropy, one is in effect straining different species of turbulence. The effect of initial anisotropy was particularly important for a symmetric flattening strain ($F = 1$, nominally). This case had not hitherto been studied and, in a sense, still has not been, since the effective type parameter is more like $F_e = 0{\cdot}5$. These vicissitudes aside, the results presented here do indicate the way in which homogeneous turbulence responds to a variety of strains, and this information should provide a number of tests for ideas concerning turbulence and a source of empirical constants for models of turbulent activity.

The experimental work was carried out under grant 9551–12 of the Defence Research Board of Canada.

REFERENCES

BATCHELOR, G. K. & PROUDMAN, I. 1954 The effect of rapid distortion of a fluid in turbulent motion. *Quart. J. Mech. Appl. Math.* **7**, 83–103.

CHAMPAGNE, F. H., HARRIS, V. G. & CORRSIN, S. 1970 Experiments on nearly homogeneous turbulent shear flow. *J. Fluid Mech.* **41**, 81–139.

COMTE-BELLOT, G. & CORRSIN, S. 1966 The use of a contraction to improve the isotropy of grid turbulence. *J. Fluid Mech.* **25**, 657–682.

DEISSLER, R. G. 1961 Effects of inhomogeneity and of shear flow in weak turbulent fields. *Phys. Fluids*, **4**, 1187–1198.

DEISSLER, R. G. 1963 Turbulent heat transfer and temperature fluctuations in a field with uniform velocity and temperature gradients. *Int. J. Heat Mass Transfer*, **6**, 257–270.

DEISSLER, R. G. 1966 Weak locally homogeneous turbulence in idealized flow through a cone. *N.A.S.A. Tech. Note*, D-3613.

DEISSLER, R G. 1967 Weak locally homogeneous turbulence and heat transfer with uniform normal strain. *N.A.S.A. Tech. Note*, D-3779.

DEISSLER, R. G. 1970 Effect of initial condition on weak homogeneous turbulence with uniform shear. *Phys. Fluids*, **13**, 1868–1869.

DOWDEN, J. M. 1972 The relaxation of stress in a ν-fluid with reference to the decay of homogeneous turbulence. *J. Fluid Mech.* **56**, 641–656.

DOWDEN, J. M. 1974 A ν-fluid model of homogeneous turbulence subjected to uniform mean distortion. *J. Fluid Mech.* **63**, 33–50.

FOX, J. 1964 Velocity correlations in weak turbulent shear flows. *Phys. Fluids*, **7**, 562–564.

HANJALIĆ, K. & LAUNDER, B. E. 1972 A Reynolds stress model of turbulence and its application to thin shear flows. *J. Fluid Mech.* **52**, 609–638.

HARLOW, F. H. & ROMERO, N. C. 1969 Turbulence distortion in a non-uniform stream. *Los Alamos Sci. Lab., University of California, Rep.* LA-4247.

HUNT, J. C. R. 1973 A theory of turbulent flow round two-dimensional bluff bodies. *J. Fluid Mech.* **61**, 625–706.

HUNT, J. C. R. & MULHEARN, P. J. 1973 Turbulent dispersion from sources near two-dimensional obstacles. *J. Fluid Mech.* **61**, 245–274.

LUMLEY, J. L. 1970 Toward a turbulent constitive relation. *J. Fluid Mech.* **41**, 413–434.

MACPHAIL, D. C. 1944 Turbulence changes in contracting and distorted passages. *Royal Aircraft Estab., Farnborough, Aero. Rep.* no. 1928.

MARÉCHAL, J. 1967*a* Disposif expérimental pour l'étude de la déformation plane de la turbulence homogène. *C.r. hebd. Séanc. Acad. Sci. Paris*, A **265**, 69–71.

MARÉCHAL, J. 1967*b* Anisotropie d'une turbulence de grille déformée par un champ de vitesse moyenne homogène. *C.r. hebd. Séanc. Acad. Sci. Paris*, A **265**, 478–480.

MARÉCHAL, J. 1972 Étude expérimentale de la déformation plane d'une turbulence homogène. *J. Mécanique*, **11**, 263–294.

MILLS, R. R. & CORRSIN, S. 1959 Effect of contraction on turbulence and temperature fluctuations generated by a warm grid. *N.A.S.A. Memo.* no. 5-5-59W.

PEARSON, J. R. A. 1959 The effect of uniform distortion on weak homogeneous turbulence. *J. Fluid Mech.* **5**, 274–288.

PROUDMAN, I. 1970 On the motion of ν-fluids. *J. Fluid Mech.* **44**, 563–603.

RIBNER, H. S. & TUCKER, M. 1953 Spectrum of turbulence in a contracting stream. *N.A.C.A. Rep.* no. 1113.

ROSE, W. G. 1970 Interaction of grid turbulence with a uniform mean shear. *J. Fluid Mech.* **44**, 767–779.

ROTTA, J. C. 1962 Turbulent boundary layers in incompressible flow. *Prog. Aero. Sci.* **2**, 1–219.

TAYLOR, G. I. 1935 Turbulence in a contracting stream. *Z. angew. Math. Mech.* **15**, 91–96.

TOWNSEND, A. A. 1954 The uniform distortion of homogeneous turbulence. *Quart. J. Mech. Appl. Math.* **7**, 104–127.

TOWNSEND, A. A. 1956 *The Structure of Turbulent Shear Flow.* Cambridge University Press.

TOWNSEND, A. A. 1970 Entrainment and the structure of turbulent flow. *J. Fluid Mech.* **41**, 13–46.

TUCKER, H. J. 1970 The distortion of turbulence by irrotational strain. *Mech. Engng Res. Lab., McGill University, Montreal, Rep.* no. 70–7.

TUCKER, H. J. & REYNOLDS, A. J. 1968 The distortion of turbulence by irrotational plane strain. *J. Fluid Mech.* **32**, 657–673.

UBEROI, M. S. 1956 Effect of wind-tunnel contraction on free-stream turbulence. *J. Aero. Sci.* **23**, 754–764.